Metrological characterization of different methods for recovering the optically sectioned image by means of structured light

P. Martinez*, C. Bermudez, G. Carles, C. Cadevall, A. Matilla, J. Marine and R. Artigas
Sensofar Tech SL, Barcelona, Spain

ABSTRACT

Imaging confocal microscopy (ICM) and focus variation (FV) are two of the most used technologies for 3D surface metrology. Both methods rely on the depth of focus of the microscope objective, which depends on its numerical aperture and wavelength of the light source to compute an optical section.

In this paper we study how several methods of structured illumination microscopy affect the metrological characteristics of an areal optical profiler. We study the effect of the projection of different structured patterns, the sectioning algorithms, and the use of high and low frequency components onto the optically sectioned image. We characterized their performance in terms of system noise, instrument transfer function and metrological characteristics such as roughness parameters and step height values.

Keywords: Focus Variation, Confocal, Optical sectioning, Structured light

1. INTRODUCTION

The most used techniques for the three-dimensional measurement of surfaces at the micro- and nanometer level are coherence scanning interferometry (CSI), imaging confocal microscopy (ICM) and focus variation (FV) [1]. While in CSI the surface height is determined by finding the location of maximum contrast of the interference along a vertical scan, in ICM and FV it is calculated detecting the maximum of intensity of the optically-sectioned images, through a function called axial response. Confocal and Focus Variation optical profilers using high numerical aperture (NA) microscope objectives are being increasingly preferred over CSI for industrial applications, because they are more robust to the environment and provide higher usability. While CSI profilers provide much higher vertical resolution independently on the magnification, they are sensitive to external vibrations that create measurement artefacts. Profilers based on focus sensing such as confocal and FV have a lower vertical resolution, but is still acceptable for most applications, and have the benefit of a reduced sensitivity to external vibrations, thus providing more robust measurements.

Confocal and FV optical profilers share a common measuring principle, that is the detection of the surface within the depth of focus of the microscope objective. The two methods scan along the optical axis, acquiring a sequence of optically-sectioned images, that are used to compute the axial response pixel-by-pixel. This axial response is then used to compute the sample's height with nanometer level resolution. However, the optical section computation of each technique is realized very differently. In FV, the sectioning is calculated by a focus operator, a mathematical computation on the image that measures the local contrast of the surface reflectivity within a set of neighboring pixels. The local contrast relies on the surface texture and is therefore problematic to calculate on smooth surfaces without texture. To avoid this issue, Bermudez [2] proposed an active illumination method to project an artificial texture onto the surface. In contrast, confocal microscopes use a set of optical and mechanical components to restrict and scan the light onto the surface, effectively calculating an axial response pixel by pixel without the influence of its neighbors, and thus preserving much better lateral resolution. Commonly, most of the commercial implementations of three-dimensional optical profilers, including those based on interferometry, implement some form of data smoothing to remove artifacts, reduce noise, and provide robust results. This smoothing slightly reduces the lateral resolution but is still sufficient to capture the features that are typically measured.

Hardware simplicity, small footprint, and cost reduction are important drivers in industrial applications and also for manufacturers that incorporate surface scanning for closed-loop manufacturing and in-line quality control. Even though FV microscopes can fulfill these demands, the lower lateral resolution and the inability to measure smooth surfaces makes them less attractive.

*pmartinez@sensofar.com; phone +34 93 700 14 92; www.sensofar.com

Classical technologies of confocal microscopy are based on laser scanning systems, disc scanning, and microdisplay scanning. Although confocal approaches have higher lateral resolution and can operate on smooth surfaces, confocal scanning laser microscopes typically have a high hardware complexity, e.g. requiring galvanometric mirrors, photodiodes, complex synchronization electronics, laser stabilization, etc. Alternatively, structured illumination microscopy (SIM)[3] provides a solution with reduced complexity. However, it is still required to scan or change in time sequence a projected pattern at the sample, normally shifting a fringe pattern. To avoid phase shifting mechanically the illumination pattern, Wicker [4] proposed a single-shot optical sectioning method by splitting the three phases of the original pattern on three different polarizations and using three cameras with properly aligned polarizers. Patorski [5] used two images, a sinusoidal pattern and a bright field to compute a π/2 shift of the original pattern with the use of the Hilbert-Huang transform. Hoffman [6] used the same idea to avoid scattering problems for in-vivo imaging, where the contrast of the pattern through scattering media decreases, and the phase shift is no longer reliable. Hoffman used a single image and recovered the bright field image by filtering the main spatial-frequency of the pattern in the Fourier space. Martinez [7] proposed a new optical arrangement in which a bright-field image and a structured-illumination image with a sinusoidal pattern are acquired and the spiral phase quadrature transform (SPQT) [8] is used to recover the optical section. The sequence of optical sections along a vertical scan was then used to recover the three-dimensional shape of the surface, showing good agreement with those acquired with a confocal profiler.

The simplicity of using an optical arrangement with a sinusoidal projection pattern and a bright field image to recover the optical section is sufficiently good for qualitative images like those used to image biological processes. However, for accurate three-dimensional profiling Martinez showed that the results on discontinuous structures, such as steps on semiconductor samples, are influenced by the single direction illumination pattern. An alternative to sinusoidal projection is using laser speckle. Ventalon [9] used a laser to illuminate a ground glass creating a volumetric speckle pattern through the sample under inspection, for fluorescence microscopy. The image recorded at the camera is the sum of the in-focus and out-of-focus components of the sample, both illuminated with contrasted speckle grains, but only the fluorescence signal from the in-focus regions retains the speckle contrast, as out-of-focus contrast is blurred. A wavelet transform is used to remove the low frequency components of the image thus leaving an optical section with a grainy appearance. In Lin [10] the same optical arrangement is used, but two images are recorded, one with the ground glass in a static position and a second one with the ground glass moving at high speed. The second image averages the speckle contrast, and thus is very close to a bright field illumination image. The two images are subtracted and low-pass filtered, resulting in an optically-sectioned image that inherently has a loss in lateral resolution. To recover high-frequency details, the bright field image is high-pass filtered and its components added to the optical section, leaving as a result an image called HiLo, very similar to a confocal image. Mazzagoni [11] analyzed the influence of the speckle contrast on HiLo image formation to optimize the optical sectioning properties. Kang [12] used the same principle of HiLo imaging using a sinusoidal pattern on an incoherent illumination microscope to record a sequence of optically-sectioned images with a high NA objective and recovering the three-dimensional shape of the surface.

In this paper we propose the design of an optical three-dimensional profiler that acquires a bright-field image and a structured illumination image. For the latter, we use a checkerboard pattern as the projected structure as, contrary to previously used sinusoidal or fringe-like patterns, has an improved directional uniformity. This configuration benefits from hardware simplicity and the associated cost reduction, and also has a higher in-plane scanning speed because only two images are recorded per scanning plane. The hardware is thus simplified to two illumination channels, one for bright field illumination and one incorporating a transmissive checkerboard glass pattern for the structured illumination. Nevertheless, for the sake of demonstration and convenience, we employed here a microdisplay scanning confocal system, which allowed us to implement both illuminations sequentially with the same channel. We implemented the system and associated reconstruction algorithms, and report here the computational factors that influence the reconstruction of the optically-sectioned images, used to reconstruct the surface. In this work, we assessed different options and parameters in each step of the proposed reconstruction algorithm, in order to explore their influence on the relevant metrological characteristics, such as system noise, instrument transfer function, accuracy, and repeatability. For this, we show the results from a series of rigorous tests using several calibration specimens such as a flat mirror, a roughness standard, a step height standard, and siemens star standard.

2. METHODS

An image recorded by the microscope is generally composed of in-focus components, with high and low spatial-frequencies, and out-of-focus components, which are blurred and only have low spatial-frequencies. In this paper we aim

to separate and recover the in-focus signal using two images at each scanning plane, one with uniform illumination, and the other one with structured illumination. This can be achieved readily using two independent illumination channels. The optically-sectioned image is recovered performing the following 4 steps:

1. Subtraction of the uniform image from the structured image
2. Computation of the contrast image
3. Blurring of the contrast image
4. Recovering the high frequency components.

The out-of-focus parts of the image also have the projected pattern but is suppressed by the defocus blur. Therefore, the first step removes the out-of-focus signal, leaving only the structured pattern projected onto the sample at the regions in focus. Results from step 1 are shown in Figure 1, where a bright field image (left) and a structured image (center) of a metallic surface were recorded using a 20X 0.45NA objective, and the subtraction image (right) shows this defocus-dependent structure, which is zero mean, except for a DC offset that is added for visualization of the structured pattern.

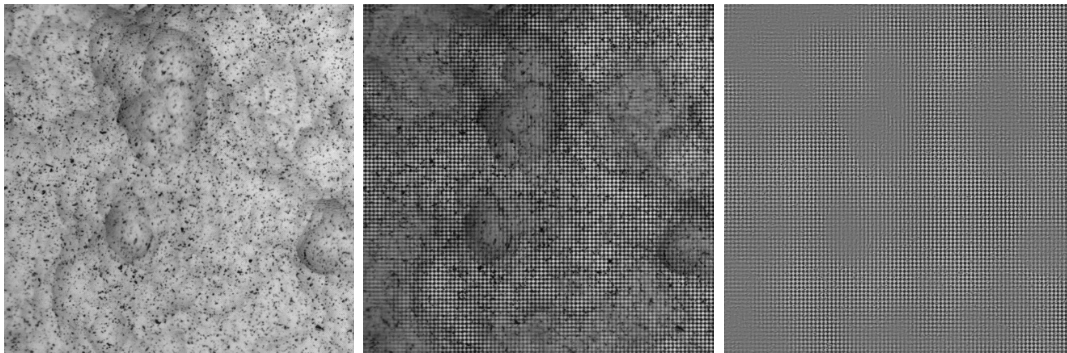

Figure 1. AIR-B40 roughness standard from NPL. Left: uniform image; center: structured image; right: subtraction image.

The results from step 1 must be converted to a contrast image, in which the in-focus parts have a high signal and the out-of-focus parts have low signal, calculated in step 2. There are multiple mathematical approaches that can be used to recover this focus-sensitive signal. In this paper we explored three different computational approaches: a square of the intensity values, a Focus Variation operator, and the spiral phase quadrature transform (SPQT). The square method basically computes the absolute value of the intensity of the difference image. The out-of-focus regions will remain near to zero values, while the in-focus regions will have much higher values. For the focus variation operator, we used a Sum of Modified Laplacian with a 5x5 pixel window. As this contrast operator relies on retrieving the optical section through neighbors' intensity contrast, it usually only works on rough samples with local intensity variations. Nonetheless, the checkerboard projected onto the sample artificially creates local texture at the in-focus regions. Finally, the SPQT relies on applying to the subtracted image from step 1 a shift of $\pi/2$ rad to all its frequencies in the Fourier space so that in combination with the original image, a contrast image can be computed. The results from applying the three mentioned methods to the image of the Figure 1 are shown in Figure 2.

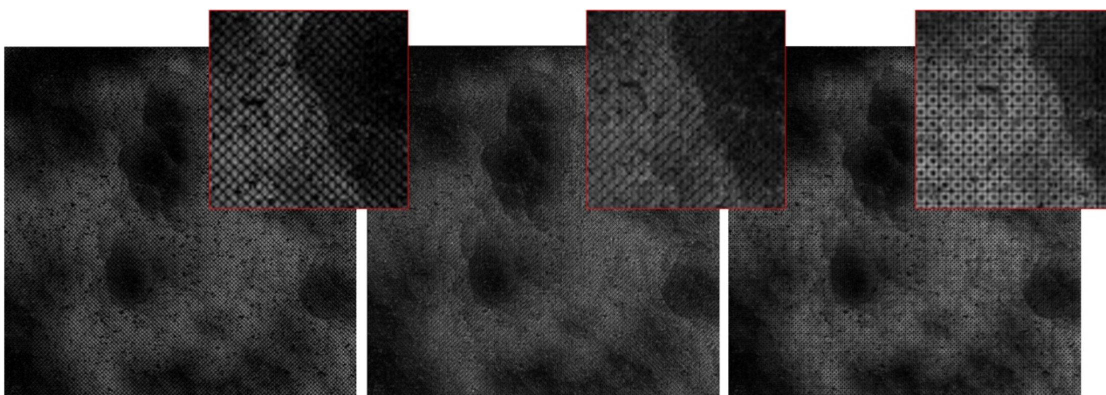

Figure 2. Contrast image. Left: squared differences; center: FV; right: SPQT.

As seen in Figure 2, all approaches are sensitive to focus, that is they provide higher signal in the in-focus regions of the sample, despite the difference in the remaining spatial structure. To remove this structure, a Gaussian blur is applied to the contrast image in step 3. Although it affects the lateral resolution, the blur provides robustness to the algorithm and minimizes the presence of spikes in the final topography, as can be seen in Figure 3. Furthermore, this loss in lateral resolution is acceptable for most applications.

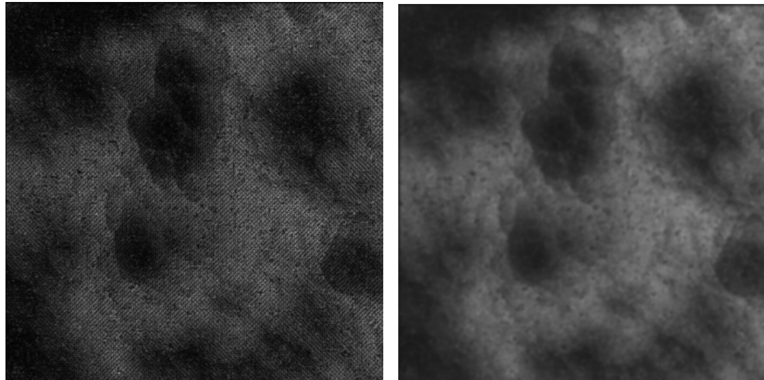

Figure 3. Left: FV contrast image; right: FV blurred contrast image.

The blurring process removes high spatial frequency information from the in-focus signal, which we intend to recover in step 4. We have analyzed two different approaches for the high-frequency recovery. The first method is through HiLo image reconstruction. This technique consists in applying a low-pass filter to the blurred image in the Fourier domain (obtaining the 'Lo' image), and a complementary high-pass filter to the uniform image (obtaining the 'Hi' image). Then the Hi and Lo images are combined in the Fourier space to provide the optically-sectioned image with high-frequency information. The second approach is a simple multiplication of the blurred image by the uniform image, one of the input images. This maintains the optical sectioning capability through the blurred image and adds high-frequency information in the in-focus signal from the uniform image. This will be referred further on as the multiplication approach. Figure 4 shows the result of applying the HiLo reconstruction method (left) and the multiplication method (right) to the blurred image from Figure 3.

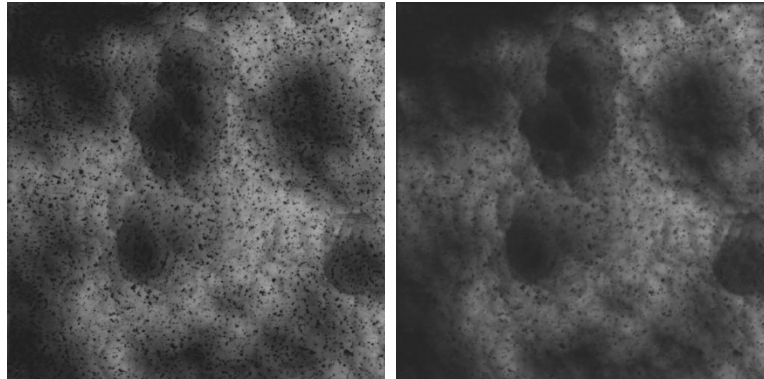

Figure 4. Left: HiLo image reconstruction; right: multiplication approach image.

Whereas the multiplication approach is computationally more efficient, it suffers from a decrease in optical sectioning capability when the sample has regions with very different reflectivity values. The low reflectivity regions decrease the optical sectioning in the multiplication method, significantly decreasing the signal to noise ratio. Instead, the HiLo approach is more robust as it works in the Fourier domain and preserves the amplitude of the low spatial frequencies independently on reflectivity variations. This effect is shown in Figure 5: whereas most of the regions within the field of view are in-focus, in the multiplication approach the final optically-sectioned image has a significant decrease in intensity in the in-focus low reflectivity region.

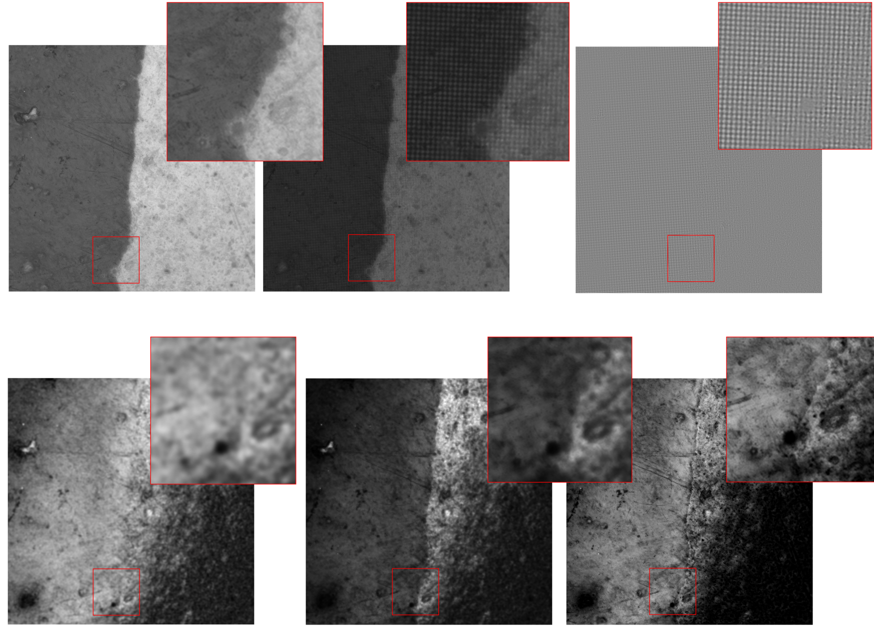

Figure 5. Top left: Uniform image; top center: structured image; top right: subtraction image; bottom left: FV contrast image; bottom center: multiplication approach; bottom right: HiLo approach.

A summary of the workflow to obtain the optically-sectioned image is shown in Figure 6.

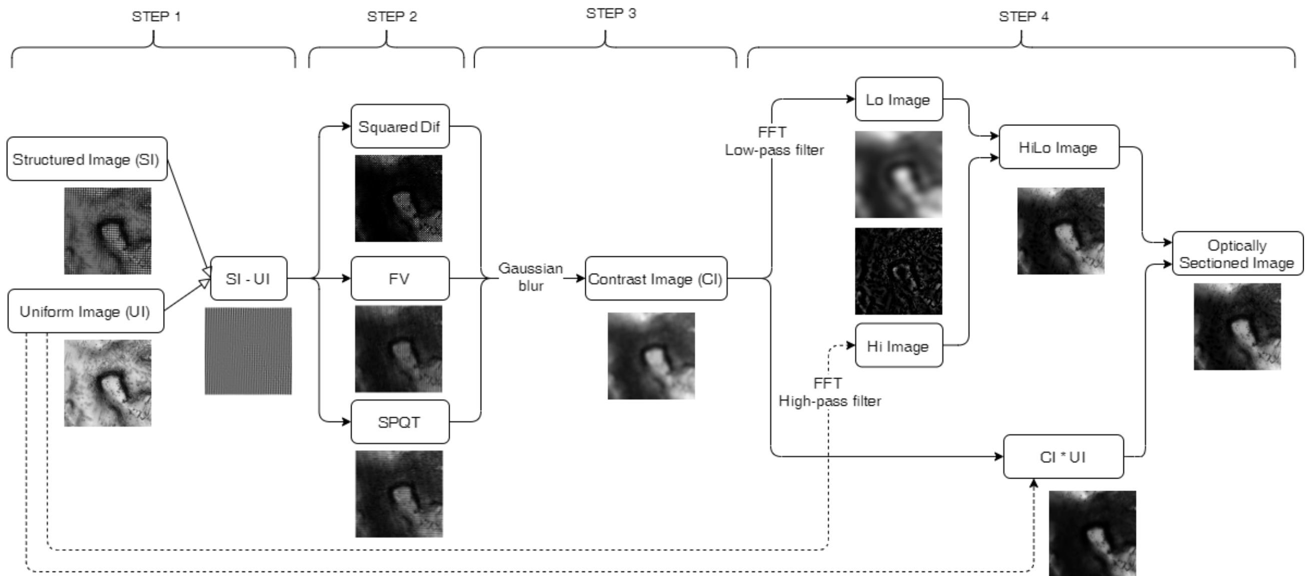

Figure 6. Workflow to retrieve the optically-sectioned image.

We propose to calculate the surface topography using a weighted sum of the blurred contrast image and the optically-sectioned image from steps 3 and 4, respectively.

We have studied the performance specification of the process of recovering the optical section as a function of the influence parameters listed in table 1, and results are shown in Section 3. We have optimized these parameters so that the system is robust for the vast majority of the samples.

Table 1. Influence parameters studied in section 3.

Step	Influence parameter	Tested values
2	Contrast algorithm	Squared Dif, FV and SPQT
3	Amount of blurring applied to the contrast image	Gaussian blur factors of 3, 6, 12 and 24 pixels
4	High-frequency recovery algorithm	Multiplication and HiLo
4	Cut-off frequency in HiLo	Cut-off frequency of 50 pixels in the Fourier domain
-	Weights in the average process before the calculation of the final topography	Average weights from 0 to 1 every 0.1

To assess the performance of the described method, several tests have been done on different types of samples. We have analyzed the system noise, height parameters on a roughness surface according to the ISO25178-3, the lateral resolution and the accuracy and repeatability from measurements of a step height standard.

3. RESULTS

For convenience and simplicity we have used a microdisplay scan confocal microscope (*S neox* optical profiler from Sensofar, Spain). The image acquisition setup for acquiring the images can be implemented through a simple optical setup, but here we benefit from a microdisplay-scan confocal microscope as it has a spatial light modulator located at the field diaphragm position. Figure 7 shows a classical arrangement of the microdisplay scan confocal microscope. The pattern encoded in the modulator is projected onto the sample, and the surface with the structured illumination is imaged at the camera. This allows to acquire the bright field and structured illumination images in time sequence, only digitally controlling the microdisplay.

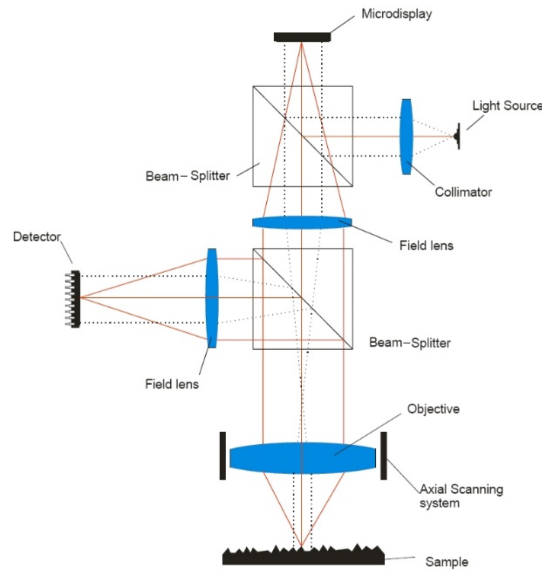

Figure 7. Optical schematic of a microdisplay scan confocal microscope.

Through the scanning, the microdisplay is programmed to project a checkerboard pattern and a bright field illumination, at each scanning plane. A sequence of optically-sectioned images are obtained using the appropriate algorithms described in the previous section, and used to reconstruct the three-dimensional surface under inspection. We observed that the checkerboard pattern has a reduced sensitivity to the spatial direction in comparison to sinusoidal projections used on a SIM microscope.

3.1 System noise

We have tested the system noise on a λ/8 SiC mirror with a 10X 0.3 NA, 20X 0.45 NA, and 50X 0.8 NA objectives. We used a reference value from a confocal optical profiler, providing a system noise of 16.5 nm, 4.9 nm and 1.2 nm for each objective respectively. The results for the three contrast methods, the two high frequency recovery methods, and four different Gaussian blurring factors are shown in Figures 8 to 10.

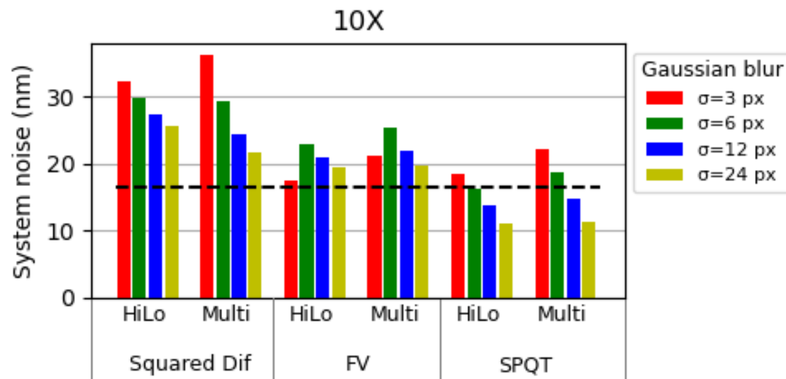

Figure 9. System noise for 10X 0.3 NA objective. Dashed line represents the reference confocal value.

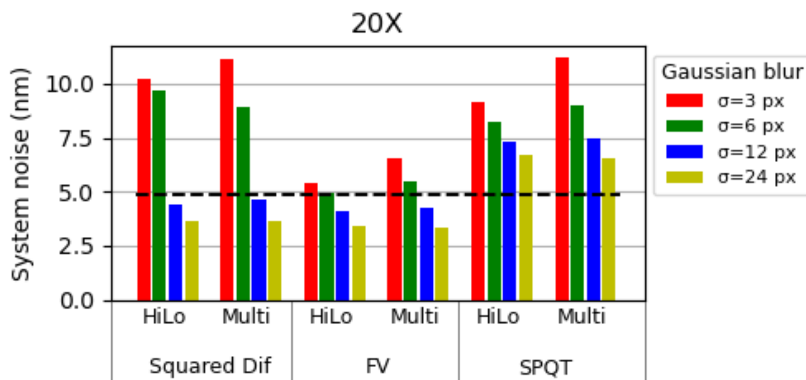

Figure 10. System noise for 20X 0.45 NA objective. Dashed line represents the reference confocal value.

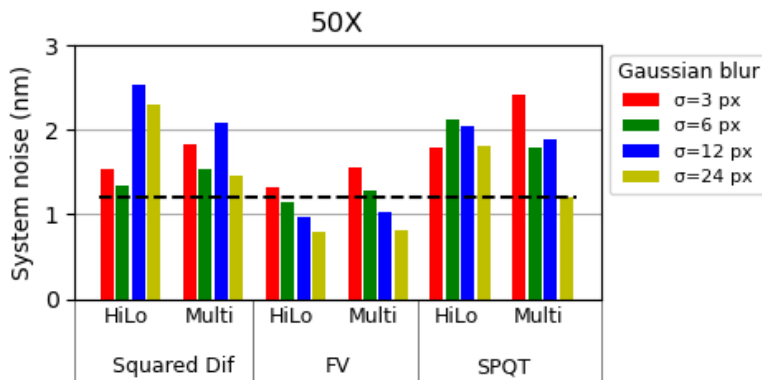

Figure 11. System noise for 50X 0.8 NA objective. Dashed line represents the reference confocal value.

Results generally show a lower system noise for larger blurring factors, which is expected since the contrast blurring is a smoothing process of the optical section, removing high frequency components of the topography. However, a greater blurring causes a decrease in lateral resolution, and so this parameter is a trade-off between these two characteristics.

Additionally, results show no significant differences between HiLo and multiplication approaches, but there are some differences between the contrast algorithms used. For instance, the FV operator provides the lowest system noise for the

20X and 50X objectives. Also, these results are comparable to the reference confocal values when using a Gaussian blur with σ equal or greater than 6 pixels.

For the 10X objective, SPQT provides slightly lower system noise than FV. This effect could be caused by a suboptimal size of the checkerboard projected at the sample, which seems to have a higher impact on the FV operator. The checkerboard pitch (physically 15.2 µm at the microdisplay) is 3.57 µm at the sample plane using the 10X objective, which corresponds to 1.6 times the Rayleigh resolution criterion (1.22λ/NA = 2.16 µm). This mismatch reduces the sectioning capability of the system because the checkerboard appears contrasted within a longer axial range, thus increasing system noise. The optimal size should match the lateral resolution criterion in order to maximize the sectioning capability whilst still preserving sufficient contrast at the in-focus planes. The checkerboard size was selected to match the lateral resolution for the higher NA objectives, which corresponds to 1.2 and 0.9 times the Rayleigh criterion for the 20X and 50X objectives respectively.

3.2 Roughness

We have measured a roughness standard (AIR-B40 from NPL, UK) with a 20X 0.45 NA objective. The post processing analysis included a least squares plane levelling, an 8 µm S-filter and a 0.8 mm L-filter. A cropped area of the results are shown in Figure 11, where the proposed method (left) is compared to a reference measurements using classical confocal and active-illumination focus variation scans. The Sq surface height parameter was then calculated and the results are shown in Figure 12. We compared the results to the confocal measurement as a value reference, which is Sq = 1.033 µm, and active illumination Focus Variation measurement, that dropped to Sq = 0.993 µm.

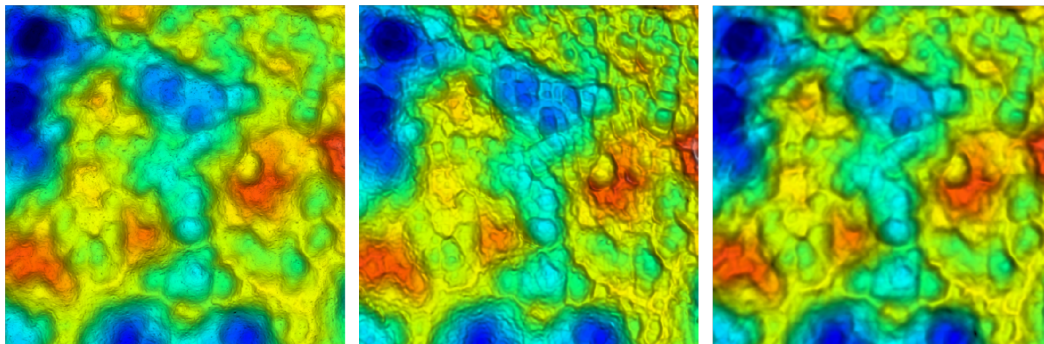

Figure 11. 300 x 300 µm crop of the Air B40 specimen. Left: HiLo with FV; center: confocal; right: AiFV.

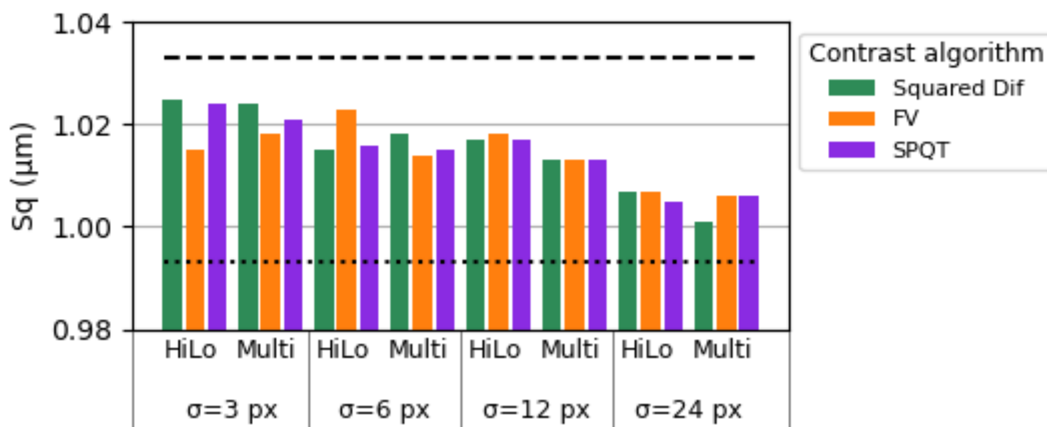

Figure 12. Sq measured on AIR-B40 roughness standard. Dashed line represents the reference confocal value while dot line represents the active illumination Focus Variation value.

Results shown in Figure 12 indicate there is no major difference between HiLo and multiplication approaches on recovering high-frequency information, nor in the contrast operator used.

As with the system noise test, it can be deducted that the higher the blurring, the lower the roughness height parameters, at the cost of sacrificing lateral resolution, as a higher blurring eliminates high-frequency information. Figure 11 shows that our proposed approach, using HiLo recovery, the high-frequency content is recovered even though a rather high blur was used to compute the topography. The frequency cut-off in the HiLo filters defined in the Fourier space was adjusted manually but could be further optimized.

3.3 Lateral resolution

To test the lateral resolution, we have measured a Siemens Star standard from NPL with a 50X 0.8 NA objective. To quantify the lateral resolution we followed the procedure described in [13]. Figure 13 shows the topography of the inner part for different Gaussian blurring factors. All measures shown were computed with a FV contrast operator and HiLo image reconstruction. The resulting lateral resolution is shown in figure 14.

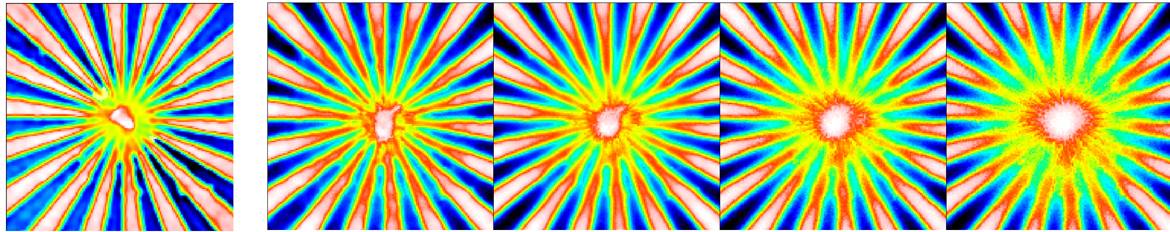

Figure 13. Central area of the Areal Siemens Star standard (left) with the reference confocal and (right) measured with FV contrast operator, using HiLo and different blurs from left to right of sigma: 3, 6, 12, and 24 pixels.

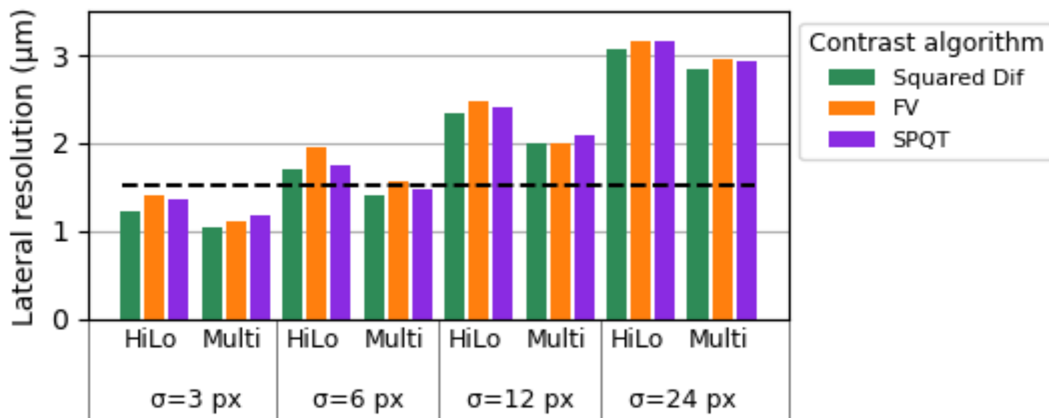

Figure 14. Lateral resolution on an Areal Siemens Star standard. Dashed lines represents the reference confocal value.

The reference confocal measurement has a lateral resolution of 1.52 µm, while the Rayleigh criterion (0.61λ/NA) for diametral lateral resolution is 0.405 µm. This difference is caused by the smoothing factors inherent in the three-dimensional reconstruction; most of the commercial implementations of three-dimensional optical profilers have some sort of smoothing to reduce noise and other factors, sacrificing a small amount of lateral resolution. This is not a problem in most of the applications, and a higher NA can be used to measure samples with smaller features. Results from the proposed method are comparable to those using the reference confocal method when using a blur of 6 pixels.

These tests also show that the multiplication approach is slightly better than HiLo reconstruction in terms of lateral resolution. This is because the low pass filter applied to the blurred contrast image adds an additional blur to the contrast image. On the other hand, the HiLo reconstruction provides more robust measurements and these are less sensitive to variations in the sample's reflectivity, which is beneficial.

As mentioned in the methods section, for the final topography we do not use directly the optically sectioned image, but a weighted average with the blurred contrast image. We have studied how different weights in the average affect the lateral resolution. Figure 15 shows the results using a Siemens Star with a 50X0.8NA objective as a function of the weight

average, for both reconstruction methods (HiLo and multiplication). A value of 1 means a weight value of 1 for the blur contrast image and 0 for the optically sectioned image.

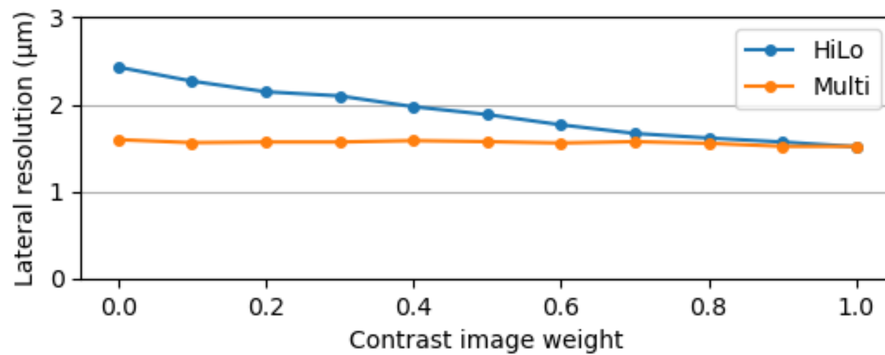

Figure 15. Lateral resolution of 50X 0.8 NA objective on an Areal Siemens Star standard using different weights of the contrast image and the optically sectioned image.

These results indicate HiLo introduces an additional blurring. Increasing the weight of the contrast image preserves information of the high frequencies. The multiplication approach does not suffer from a loss in lateral resolution because the optical sectioning capability is unchanged. Nevertheless, a contrast image weight lower than unity provides more robust HiLo measurements, in particular on measuring samples with low contrast or high variations in reflectivity, and so the small drop in lateral resolution is in general acceptable.

In all, it can be concluded that using the focus variation operator with a Gaussian blur of 6 pixels in combination with HiLo has a good compromise, with low system noise, good lateral resolution and robustness to measure samples with high reflectivity variations.

3.4 Step height

Finally, we have tested the performance measuring a step height standard (model SHS-8.0 QC from VLSI, USA), with a 20X 0.45 NA objective. The post processing included a least square levelling, mean profile extraction, and evaluating the step height according to ISO 5436-1:2000, section 7.1.

We performed 100 independent measurements and obtained a mean value of the step height of 7.616 µm and a repeatability of 6.8 nm, which is 0.09% of the step height. The calculations included an amplification factor of 0.973 obtained according to ISO 25178-700.

4. CONCLUSIONS

We have shown an image reconstruction method of an optically sectioned image for the three-dimensional measurement of surfaces. The method only requires acquiring two images: a uniform bright field image and a structured illumination image using a checkerboard pattern. We have shown three different methods to evaluate the contrast of the projected pattern (square of intensities, FV, and SPQT), and two different methods to recover high spatial-frequency components of the image (multiplication and HiLo). The parameters of the image reconstruction method influence the metrological characteristics. We have evaluated the performance specification with a set of different parameters with emphasis on the system noise, lateral resolution, and accuracy of measurements on a roughness and step height standard specimens. The combination of a FV algorithm and HiLo reconstruction appeared to be a robust and consistent method for measuring a wide range of samples. Further optimization of the HiLo filters, such as the selected cut-off frequencies, could improve the performance of the method, in particular in terms of lateral resolution.

REFERENCES

[1] Leach R. "Optical Measurement of Surface Topography". Springer Verlag ISBN 978-3-642-12012-1

[2] Bermudez C., Martinez P., Cadevall C., Artigas R., "Active Illumination Focus Variation". Proc. SPIE 11056, Optical Measurement Systems for Industrial Inspection XI, 110560W (21 June 2019).

[3] M. A. A. Neil, R. Juškaitis, and T. Wilson. "Method of obtaining optical sectioning by using structured light in a conventional microscope". Vol. 22, No. 24 / OPTICS LETTERS (1997).

[4] Kai Wicker and Rainer Heintzmann. "Single-shot optical sectioning using polarization-coded structured illumination".J. Opt. 12 084010 (2010).

[5] Krzysztof Patorski, Maciej Trusiak, and Tomasz Tkaczyk. "Optically-sectioned two-show structured illumination microscopy with Hilbert-Huang processing". Optics Express 9517, Vol. 22, No. 8 (2014).

[6] Zachary R. Hoffman, Kose Kivanc, Charles A. DiMarzio. "Single image structured illumination (SISIM) for in-vivo imaging". Proc. SPIE 10499, Three- Dimensional and Multidimensional Microscopy: Image Acquisition and Processing XXV (2018).

[7] Martinez P., Bermudez C., Cadevall C., Marilla A., Artigas R. "Three-dimensional Imaging Confocal profiler without in-plane scanning". Proc SPIE 113520L, Optics and Photonics for Advanced Dimensional Metrology (2020).

[8] Kieran G. Larkin. "Natural demodulation of two-dimensional fringe patterns. I. General background of the spiral phase quadrature transform". J. Opt. Soc. Am. A/Vol. 18, No. 8 (2001).

[9] Ventalon C., Heintzmann R., Mertz J. "Dynamic speckle illumination microscopy with wavelet prefiltering". Vol. 32, No. 11 / OPTICS LETTERS (2007).

[10] Lim D., Ford, T., Chu K., Mertz J. "Optically sectioned in vivo imaging with speckle illumination HiLo microscopy". Journal of Biomedical Optics 16 (1), 016014 (2011).

[11] Mazzaferri J., Kunik D., Belisle J.M., Singh K., Lefrançois S., Constantino S. "Analysing speckle contrast for HiLo microscopy optimization. Optics Express, Vol 19, Issue 15, pp 14508-14517 (20119

[12] Kang S., Ryu I., Kim D., Kauh S.K. "High-speed three-dimensional surface profile measurement with the HiLo optical imaging technique. Optics and Photonics, Vol. 2, No. 6, pp 568-575 (2018).

[13] Giusca C., Leach R., Helery F. "Good practice guide nº 128. Calibration of the metrological characteristics of Imaging Confocal Microscopes (ICMs). National Physics Laboratory (2013).